Journal of the Korean Nuclear Society
Volume 28, Number 2, April 1996

Analysis of the Mean Uranium Valence of $U_{1-y}Er_yO_{2\pm x}$ Solid Solutions in terms of Lattice Parameter and Oxygen Potential

Han Soo Kim and Dong Seong Sohn
Korea Atomic Energy Research Institute
(Received September 20, 1995)

격자상수 및 산소포텐샬에 의한 $U_{1-y}Er_yO_{2\pm x}$ 고용체의 평균우라늄원자가 분석

김한수 · 손동성
한국원자력연구소
(1995. 9. 20 접수)

Abstract

The lattice parameters of stoichiometric UO_2 and $U_{1-y}Er_yO_2$ in the range of $y=0.01$ to $y=0.33$ were determined with use of X-ray diffraction data. Oxygen potentials have been measured by means of a thermogravimetric method in the range of 1200~1500°C and $10^{-14} \leq p_{O_2} \leq 10^{-3}$ for pure UO_2 and $U_{1-y}Er_yO_{2\pm x}$ solid solutions with $y=0.02$, $y=0.06$ and $y=0.20$, respectively. Their oxygen partial pressures were maintained by controlling CO_2/CO mixture atmosphere, and the p_{O_2} values corresponding to x of $U_{1-y}Er_yO_{2\pm x}$ solid solutions were measured with an electrolyte oxygen sensor.

The lattice parameter decreases linearly with an increase in the erbium content. The change of the lattice parameter can be expressed in a linear equation of y as $a(\text{Å}) = 5.4695 - 0.220y$ for $0 \leq y \leq 0.33$. The experimental coefficients of $y=-0.220$ in $U_{1-y}Er_yO_2$ was an intermediate value between the calculated values -0.273 and -0.156 in the case of U^{5+} and U^{6+}, respectively.

The $\Delta \overline{G}_{O_2}$ has been found to undergo abrupt increase in the range of -360 to -270 kJ/mole for $y=0.06$ and -320 to -220 kJ/mole for $y=0.20$, respectively, in the temperature range of 1200~1500°C. $\Delta \overline{G}_{O_2}$ increases with erbium content, but the effect of the dopant for $x=0.01$ is less significant than that for stoichiometry.

The oxygen potentials for UO_2 and $U_{0.98}Er_{0.02}O_{2+x}$ can be approximately represented by the U^{5+}/U^{4+} model but those for $y \geq 0.06$ in $U_{1-y}Er_yO_{2\pm x}$ solid solutions cannot be interpreted by the mean uranium valence model.

요 약

$0 \leq y \leq 0.33$ 범위의 조성을 가진 $U_{1-y}Er_yO_{2\pm x}$ 고용체의 격자상수를 least-squares method에 의해 구하였다. 고용체의 격자상수는 Er의 첨가량이 증가함에 따라 다음과 같이 직선적으로 감소하였다 : $a(\text{Å}) = 5.4695 - 0.220y$, $(0 \leq y \leq 0.33)$. $U_{1-y}Er_yO_{2\pm x}$ 고용체에서 Er 함량에 대한 격자상수의 변화계수,

y=−0.220은 Er^{3+}의 첨가에 따른 전기적 중성을 만족하기 위해 고용체내에서 U^{5+} 또는 U^{6+} 이온이 각각 존재한다고 가정하여 계산된 값, y=−0.273, −0.156의 사이에 있다.

$U_{1-y}Er_yO_{2\pm x}$ 고용체와 UO_{2+x}의 산소포텐샬을 산소분압 $10^{-14}-10^{-3}$, 온도 1200~1500°C에서 thermogravimetric method에 의해 측정하였다. CO_2/CO 혼합가스로써 TGA내의 산소분압을 조절하였으며, 고온산소센서를 사용하여 p_{O_2} 값을 측정하였다. $\Delta \bar{G}_{O_2}$ 값은 1200~1500°C 범위에서 y=0.06인 고용체의 경우 −360부터 −270 kJ/mole, 그리고 y=0.20인 고용체에서는 −320부터 −220 kJ/mole 까지 각각 급격하게 변하는 것으로 나타났다.

$U_{1-y}Er_yO_{2\pm x}$ 고용체에서 Er의 함량이 낮은 경우에는 U^{5+}/U^{4+} model이 산소포텐샬 데이타에 접근하는 것으로 나타났으나, y=0.06 이상인 경우에는 평균 우라늄 원자가모델에 의해서 산소 포텐샬의 변화를 설명할 수 없었다.

1. Introduction

Erbium is considered as slow burning absorber suitable for use in a PWR fuel management scheme for high burnup and/or extended cycle operation [1]. It is important to consider thermodynamic properties of erbium doped fuel in addition to its neutronic properties. Uranium dioxide is known to accommodate erbium ions, forming solid solutions of the type $U_{1-y}Er_yO_{2\pm x}$ during sintering of Er-doped UO_2 pellets at high temperature. Therefore, the addition of dopant to UO_2 matrix influences the lattice structure and thermodynamic properties due to the differences in charge and size of the cation. Well defined thermodynamic data of $U_{1-y}Er_yO_{2\pm x}$ are required for better understanding of thermal and irradiation behaviors of Er-doped fuel.

Thermal processes of the oxide system such as sintering and creep at high temperature is mainly controlled by the uranium diffusivity which is related to the mean uranium valence. The mean uranium valence of $U_{1-y}Er_yO_{2\pm x}$ solid solutions can be found from the change of lattice parameter with dopant content. It can be also deduced from the relation between mean uranium valence and oxygen potential. The most reasonable valence can be determined from the degree of agreement between measured oxygen potentials and calculated values from the mean uranium valence models.

The oxygen potentials of $UO_{2\pm x}$ and that of UO_2 doped with various foreign cations have been reported by previous investigators [2-19]. Kim et. al., [20] have reported the oxygen potentials of the $U_{1-y}Er_yO_{2\pm x}$ solid solutions. In this study, further experimental work has been done to obtain the thermodynamic data for y=0.02 and the supplementary data for y=0.06 and 0.20 in high p_{O_2} region.

In the case of the M^{m+} ions with m<4 substituting U^{4+} ions of UO_2, oxygen potential generally increases and the uranium atoms are oxidized to a mean uranium valence higher than 4+, unless the corresponding amount of oxygen vacancies is formed in the anion sublattice resulting from neutrality condition. According to Ohmichi et al.[21], the lattice parameter change with y in $U_{1-y}Gd_yO_{2+x}$ can be interpreted by considering that the accommodation of one atom Gd^{3+} causes oxidation of one U^{4+} atom in the crystal to U^{5+} in the composition range where the mean valence of uranium is between 4+ and 5+. If this holds also for the present $U_{1-y}Er_yO_{2+x}$ solid solutions, the uranium ions will be oxidized first to U^{5+} from U^{4+} and then to U^{6+} from U^{5+} by introducing further Er atoms.

In the present paper, the lattice parameters of pure UO_2 and the $U_{1-y}Er_yO_{2\pm x}$ solid solutions with erbium content in the range of $0.01 \le y \le 0.33$ were determined. The oxygen potentials of UO_2 and the $U_{1-y}Er_yO_{2\pm x}$ solid solutions with y=0.02, y=0.06 and y=0.20 have been measured in the temperature range of 1200~1500°C, respectively, by the thermog-

ravimetric method using CO_2/CO mixtures for controlling the p_{O_2} in the gas phase. The mean uranium valence of the $U_{1-y}Er_yO_{2\pm x}$ solid solutions is analyzed in terms of the lattice parameters and oxygen potentials.

2. Experimental Methods and Materials

2.1. Sample Preparation

Powder samples were prepared for thermogravimetric studies by mechanical blending of $UO_{2.099}$ with weighed amount of Er_2O_3 powder for 4 hours. UO_2 powder having total impurities of less than 200ppm was obtained by the ammonium uranyl carbonate (AUC) conversion process where AUC precipitates were pyrohydrolized and calcined in wet hydrogen gas at 650°C. Er_2O_3 powder having the metallic purity of 99.99% was supplied from the Aldrich Chemical Co., Ltd. The impurity contents of UO_2 and Er_2O_3 powders are shown in Table 1.

Mixed powder samples, which were mixed using inclined cylindrical mixer, were pressed at 286MPa into green pellets of about 15mm in diameter and 9 mm in length, which were then sintered at 1850°C in hydrogen gas for 4hours. The sample preparation procedure is intended to ensure that true solid solutions are obtained. Sintered pellets were encapsuled in quartz tubes in vacuum and homogenized at 1000°C for 405 hours. The pellets were then crushed into chips, and used for thermogravimetric measurements.

2.2. X-ray Diffraction Measurements

The homogenized pellets were sliced, polished and annealed to obtain the stoichiometric composition at 1200°C in $p_{O_2}=10^{-11.2}$, and then used for x-ray diffraction specimens. X-ray diffraction measurements of the solid solutions were made with use of a diffractometer with Cu-Kα radiation. Lattice parameters were determined by the least-squares method.

Table 1. Impurity Contents of UO_2 and Er_2O_3 Powders

UO_2 powder			
U content : 87.72%			
H_2O : 0.22%			
O/U ratio : 2.099			
Impurities (ppm U basis) :			
Al	< 10	B	< 0.2
C	60	Ca	< 20
Cd	< 0.2	Cr	<10
Cu	< 10	Dy	< 0.1
F	2.8	Fe	< 50
Gd	< 0.1	Mg	< 10
Mn	< 5	Mo	< 1
Ni	< 10	Si	< 10
Th	< 100		
Er_2O_3 powder			
Erbium (Ⅲ) oxide : 99.99%			
Er content : 87.3%			
Impurities (ppm Er basis) :			
Rare earth elements : none detected			
Mg	45 ppm		
Cr	25 ppm		
Zr	20 ppm		
Ca	5 ppm		

2.3. Thermogravimetric Measurements of $\Delta \overline{G}_{O_2}$

The thermogravimetric method of measuring equilibrium oxygen pressures is based upon weight change of a sample. As shown in Fig. 1, the thermogravimetric apparatus is constructed with use of Setaram model TGA 92 that has an electronic microbalance with the sensitivity of 1μg. The balance was connected with a carrier gas and auxiliary gas supply system, and with a graphite resistance furnace with an alumina work tube. The sample was placed in a Pt crucible, and it was suspended from the balance by a Pt-Rh wire into the work tube.

Thermogravimetric measurements were performed under the oxygen partial pressures of 10^{-14} to 10^{-3} for pure UO_2 and for three Er compositions, namely, $y=0.02$, $y=0.06$ and $y=0.20$ in $U_{1-y}Er_yO_{2\pm x}$ solid solutions at the temperature range of 1200~1500°

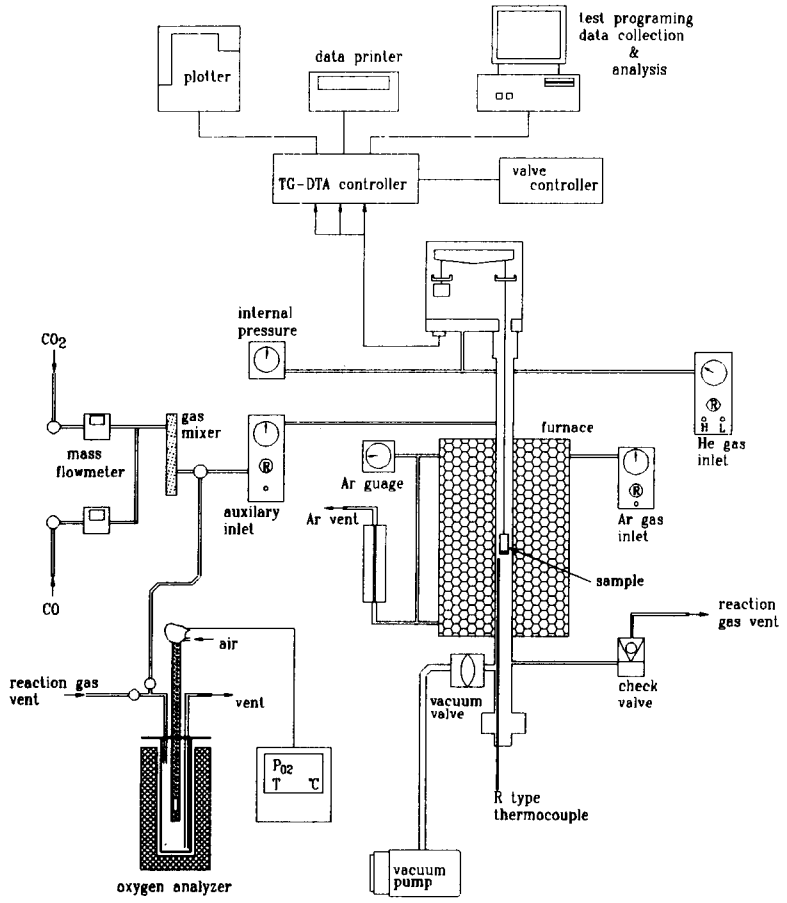

Fig. 1. Experimental Apparatus of Thermogravimetric Measurement.

C. The oxygen partial pressure was controlled within ±0.03 of log p_{O_2} value by adjusting CO_2/CO mixing ratio with calibrated digital mass flowmeters. The purities of both CO_2 and CO gases were higher than 99.99%. The oxygen partial pressure was checked by an oxygen probe inserted in the fixed-temperature furnace that is connected to the inlet of the TGA furnace. The value of oxygen partial pressure was obtained from the sensor voltage E (mV) using the Nernst's equation as follows ;

$$\log p_{O_2,\,sen} = p_{O_2,\,ref} - \frac{E}{0.0496\ T_{sen}}, \quad (2-1)$$

where $p_{O_2,\,sen}$ is the oxygen partial pressure measured by the sensor, $p_{O_2,\,ref}$ the oxygen partial pressure of reference gas ($p_{O_2,\,ref}$ =0.206 atm at air of 1 atm.), T_{sen} sensor temperature.

For the reaction $CO+{}^1/_2O_2 = CO_2$, equilibrium constant at oxygen sensor is

$$K_{sen} = 10^A = \frac{p_{CO,\,sen}\ p_{O_2^{1/2},\,sen}}{p_{CO_2,\,sen}}, \quad (2-2)$$

where $A=-14{,}749/T_{sen}+4.534$. The equilibrium constant at TGA furnace is

$$K_{TGA} = 10^B = \frac{p_{CO,\,TGA}\ p_{O_2^{1/2},\,TGA}}{p_{CO_2,\,TGA}}, \quad (2-3)$$

where $B=-14{,}749/T_{TGA}+4.534$ and T_{TGA} is the temperature of TGA furnace. Since CO_2/CO ratio at inlet of TGA is nearly the same as that at inlet of sensor furnace, the oxygen partial pressure at TGA

furnace is

$$p_{O_2,TGA}^{1/2} = 10^B \frac{p_{CO_2,TGA}}{p_{CO,TGA}} = \frac{10^B}{10^A p_{O_2,sen}^{1/2}}. \quad (2-4)$$

From Eq.(2−1) and Eq.(2−4), the oxygen partial pressure of TGA furnace is given by the following equation :

$$\log p_{O_2,TGA} = 29,498 \left(\frac{1}{T_{sen}} - \frac{1}{T_{TGA}}\right) - \left(\frac{20.158\ E}{T_{sen}} + 0.686\right). \quad (2-5)$$

The potential $\Delta \bar{G}_{O_2}$ value is obtained as follows :

$$\Delta \bar{G}_{O_2}(J/mole) = 2.303\ RT_{TGA} \log p_{O_2,TGA}. \quad (2-6)$$

For in-situ determination of the oxygen to metal ratio by the thermobalance, it is necessary to adjust the oxygen composition to produce stoichiometric reference state. It is assumed that a straight line in the curve of $\Delta \bar{G}_{O_2}$ versus relative weight change corresponds to the stoichiometric composition. The values of the O/(U+Er) ratio at various oxygen potentials and temperatures were calculated from weight changes relative to the reference state as follows :

$$\frac{O}{U+Er}\ ratio = 2 + \left\{\frac{W_M (W_1 - W_2)}{16\ W_2}\right\}, \quad (2-7)$$

where W_M is the molecular weight of stoichiometric dioxide, W_1 is the weight of sample, and W_2 is the weight after conversion to the reference state.

3. Results and Discussion

3.1. Phase Relations

The oxygen to metal ratios of $U_{1-y}Er_yO_2$ solid solutions sintered in hydrogen atmosphere are considered to be below 2.00 since the oxidation state of dissolved Er in UO_2 cannot exceed the ionic valence +3. Therefore, x-ray specimens were annealed to obtain the stoichiometric composition at 1200°C in $p_{O_2} = 10^{-11.2}$ after homogenization treatment. Une and Oguma [15] analyzed the oxygen to metal ratios of $U_{1-y}Er_yO_2$ solid solution pellets sintered in hydrogen atmosphere at 1700°C, by a spectrophotometric method. The results showed that the O/(U+Gd) ratios of all pellets were in the narrow range of 1.995 to 2.000, being independent of $GdO_{1.5}$ content with $0.04 \le y \le 0.27$ and averaged to be 1.997, just below the stoichiometric composition. However, Beals and Handwerk [22] analyzed chemically the oxygen to metal ratios of urania-gadolinia solid solutions sintered in hydrogen and argon atmospheres, and found that the O/(U+Gd) ratios were about 2.00 up to 40 mole % Gd cations.

The change of lattice parameter of the $U_{1-y}Er_yO_2$ solid solution is plotted as a function of dopant content in Fig. 2, where comparison was made with other similar solid solutions. It can be noticed that, for all the solid solutions, the lattice parameters decrease linearly with the increase of the dopant content, and the trend of parameter change of $U_{1-y}Er_yO_2$ was similar to that of $U_{1-y}Y_yO_2$ solid solution. The break in the lattice parameter of the $U_{1-y}Er_yO_2$ solid solutions has not found in the range of y=0 to y=0.33. The change of lattice parameter as a linear equation is expressed as

$$a(\text{Å}) = 5.4695 - 0.220y \text{ for } x=0,\ 0 \le y \le 0.33. \quad (3-1)$$

The linearity shows that the solid solutions exist in a single phase and the crystal structure is the same as UO_2 structure up to y=0.33.

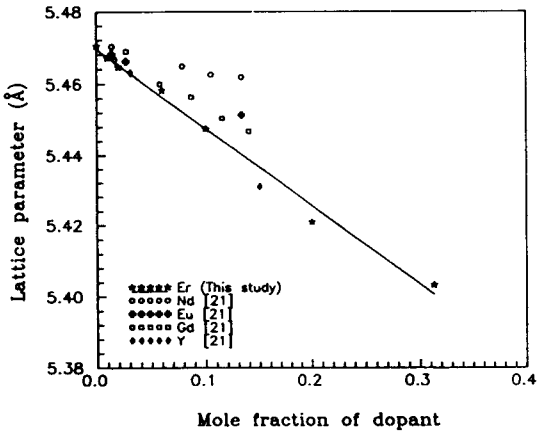

Fig. 2. Lattice Parameters of $U_{1-y}M_yO_2$ Solid Solutions versus Mole Fraction of Dopants.

When Er^{3+} is substituted for U^{4+} ion in the cation lattice, either an oxygen vacancy is created or some of the U^{4+} ions are oxidized to U^{5+} or U^{6+} to meet electroneutrality conditions. Using a simple ionic model, Ohmichi et al. [21] explained the rate of change of lattice parameter with y in $M_yU_{1-y}O_{2+x}$ solid solutions. It is found that the oxidation state of uranium is U^{5+} rather than U^{6+} in the low concentration range of rare earth elements. By applying the model to the present case, the following two equations were derived according to the resultant oxidation states of uranium, U^{5+} and U^{6+}, by the incorporation of Er^{3+}.

In the case of U^{5+}, the chemical form of the solid solution is described as $U^{4+}_{1-2y}U^{5+}_y\ Er^{3+}_y\ O^{-2}_2$. The lattice parameter is given as

$$a(\text{Å}) = \frac{4}{\sqrt{3}}\{(1-2y)\ r_{U^{4+}} + y\ r_{U^{5+}} + y\ r_{Er^{3+}} + r_{O^{2-}}\}. \quad (3-2)$$

By differentiating the lattice parameter with y,

$$\frac{da}{dy} = \frac{4}{\sqrt{3}}(r_{Er^{3+}} + r_{U^{5+}} - 2\ r_{U^{4+}}). \quad (3-3)$$

In the case of U^{6+}, the chemical form is $U^{4+}_{1-3y/2}U^{6+}_{y/2}\ Er^{3+}_y\ O^{-2}_2$. So, da/dy is obtained in a similar way as

$$\frac{da}{dy} = \frac{4}{\sqrt{3}}(r_{Er^{3+}} + \frac{1}{2}\ r_{U^{6+}} - \frac{3}{2}\ r_{U^{4+}}), \quad (3-4)$$

where $r_{Er^{3+}}$, $r_{U^{4+}}$, $r_{U^{5+}}$ and $r_{U^{6+}}$ are the ionic radii of the respective ions for eight-coordination and $r_{O^{2-}}$, which is not a function of y, is an effective radius of oxygen.

The coefficients of y in $U_{1-y}Er_yO_2$, which were calculated by above Ohmichi's approach and by taking 1.004 Å for eight-coordination effective ionic radius of Er^{3+} [23], were −0.273 and −0.156 for the oxidation state of U^{5+} and U^{6+}, respectively.

Table 2. Comparison of the Coefficients of y

Ion	Radius(Å)	Experimental da/dy	Calculated da/dy	
			U^{5+} state	U^{6+} state
O^{2-} CN=4	1.368			
U^{4+} CN=8	1.001			
U^{5+} CN=8	0.880	−0.220	−0.273	−0.156
U^{6+} CN=8	0.860			
Er^{3+} CN=8	1.004			

As shown in Table 2, the experimental coefficient of y=−0.220 was an intermediate value between the calculated values −0.273 and −0.156 in the case of U^{5+} and U^{6+}, respectively. It shows indirectly the coexistence of U^{5+} and U^{6+} in the $U_{1-y}Er_yO_2$ solid solutions for $y \leq 0.33$.

3.2. Oxygen Potentials of $U_{1-y}Er_yO_{2\pm x}$ Solid Solutions

The oxygen potentials of $U_{1-y}Er_yO_{2\pm x}$ solid solutions against O/(Er+U) ratio are presented in Fig. 3, Fig. 4 and Fig. 5 for the Er mole fractions of y=0.02, y=0.06 and 0.20, respectively. Fig. 3 shows that the $\Delta\overline{G}_{O_2}$ values for $U_{0.98}Er_{0.02}O_{2\pm x}$ solid solutions are higher than that for pure UO_{2+x}. The plots of $\Delta\overline{G}_{O_2}$ against O/(U+Er) ratio show the expected increase in oxygen potentials as the oxygen to metal ratio goes to hyperstoichiometric composition. From the slopes of the plots of $\Delta\overline{G}_{O_2}$ against O/(U+Er) ratio, it is found that $\Delta\overline{G}_{O_2}$ increases more rapidly at 1500°C than the two of lower temperatures. A very rapid change in $\Delta\overline{G}_{O_2}$ is observed in Fig. 3, Fig. 4 and Fig. 5, when the composition deviates from stoichiometry to hyperstoichiometry.

$\Delta\overline{G}_{O_2}$ has been found to undergo an abrupt increase in the ranges of −270 to −360 kJ/mole for y=0.06 and −220 to −320 kJ/mole for y=0.20, respectively, in the temperature range of 1200~1500°C. No data are available on $\Delta\overline{G}_{O_2}$ for $U_{1-y}Er_yO_{2\pm x}$ to be compare with the present data. K. Une et al.[10] suggested that the exactly stoichiometric $U_{0.86}Nd_{0.14}O_2$ and $U_{0.73}Nd_{0.27}O_2$ exist in relatively small ranges of −240 to −280 kJ/mole and −180 to −230 kJ/mole, between 1000 and 1500°C, respectively. The oxygen potentials of $U_{1-y}Er_yO_{2\pm x}$ increase positively with increasing Gd content and the steepest change in $\Delta\overline{G}_{O_2}$ occurs at O/M=2.00. The $\Delta\overline{G}_{O_2}$ values are −50 to −65 kcal/mole at stoichiometric composition for y=0.14, and −58 and −43

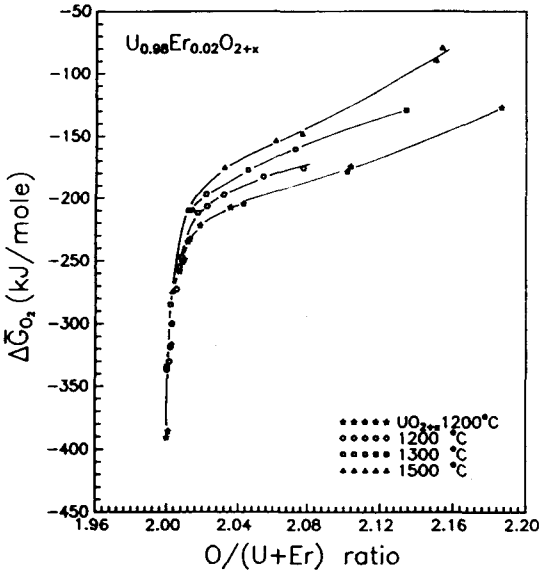

Fig. 3. Oxygen Potentials of $U_{0.98}Er_{0.02}O_{2\pm x}$ Solid Solutions at 1200, 1300 and 1500°C.

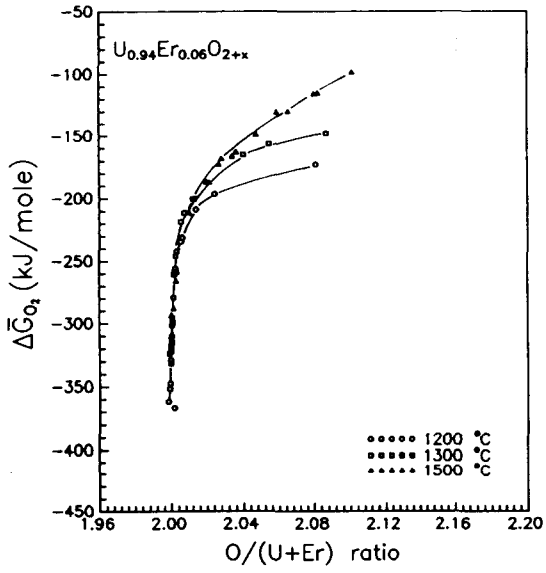

Fig. 4 Oxygen Potentials of $U_{0.94}Er_{0.06}O_{2+x}$ Solid Solutions at 1200, 1300 and 1500°C.

kcal/mole at 1000 and 1500°C, respectively, for y=0.27 [14, 15].

Hypostoichiometric phase is appeared for y=0.20, as shown in Fig. 5. It shows that an addition of Er cations in UO_2 remarkably stabilizes the oxygen de-

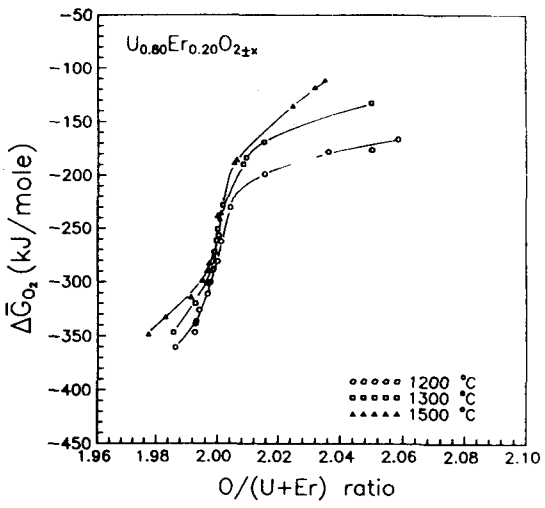

Fig. 5 Oxygen Potentials of $U_{0.80}Er_{0.20}O_{2\pm x}$ Solid Solutions at 1200, 1300 and 1500°C.

ficient part of the solid solutions. This stabilization trend in the hypostoichiometric phase by foreign cation additions to UO_2 has been reported on the solid solutions of Gd [15], Mg [24], Nd [10], Ce [8], Pu [18, 19], Pr [9] and Eu [12]. Divalent Mg ion appears to have a much larger effect on the change in $\Delta\bar{G}_{O_2}$ value than trivalent Gd and Nd ions.

It is regarded that the O/(U+M) ratio giving the steepest change in $\Delta\bar{G}_{O_2}$ is exactly 2.0 which is true for $U_{1-y}M_yO_{2+x}$ with M^{4+} but does not seem to have been corroborated as exactly true for those with M^{3+} and/or M^{2+}. The shift to a lower O/(U+M) ratio than 2.0 has been observed for the solid solution containing divalent Mg [25], Eu [12] and Sm [11]. The steepest change of the oxygen potential in $U_{1-y}M_yO_{2\pm x}$ occurs at O/(U+Eu) ratios less than 2.0, namely 1.983 for y=0.1 and 1.950 for y=0.3, and O/(U+Mg)=1.991 for y=0.05 at 1000°C. Lindemer and Sutton [13] note that if the O/(Gd+U) ratio is set to 2.0 at $\Delta\bar{G}_{O_2}=-287$ kJ/mole at 1500°C for $U_{1-y}Gd_yO_{2+x}$ as for UO_{2+x}, the nearly vertical portion of $\Delta\bar{G}_{O_2}$ data shifts with increasing to higher oxygen potentials. These observations are not consistent with results reported for the most other solid solutions containing trivalent lanthanides. It has been reported

that hypostoichiometric $U_{1-y}M_yO_{2-x}$ solid solutions are very readily oxidized to stoichiometric composition during the furnace cooling in 10^{-1} Pa vacuum or standing in air at room temperature, so that the oxygen composition in equilibrium can not be determined [21, 26]. However, the precise determination of the O/(U+M) ratio, where the steepest change of oxygen potentials occurs with oxygen composition, is essential for the use of the reference of the compositon in $\Delta \bar{G}_{O_2}$ measurements.

The $\Delta \bar{G}_{O_2}$ values as a function of erbium content for x=0.00 and x=0.01 in $U_{1-y}M_yO_{2-x}$ $U_{1-y}Er_yO_{2+x}$ solid solutions at 1200, 1300 and 1500°C are shown in Fig. 6. It is shown that the $\Delta \bar{G}_{O_2}$ values increase with erbium content, but the effect of dopant content for x=0.01 is less significant than that for stoichiometry. A clear relation between erbium content and magnitude of the difference in $\Delta \bar{G}_{O_2}$ for x=0.01 is not observed.

3.3. Mean Uranium Valence in $U_{1-y}Er_yO_{2\pm x}$

It has been known that the oxygen potential of hyperstoichiometric phase of fluorite solid solution can be interpreted by the change of uranium valence state [16, 26]. If dopant cation has a stable 3+ valence, the deviation of solid solution from exact stoichiometry must be permissible because the uranium has many valence states.

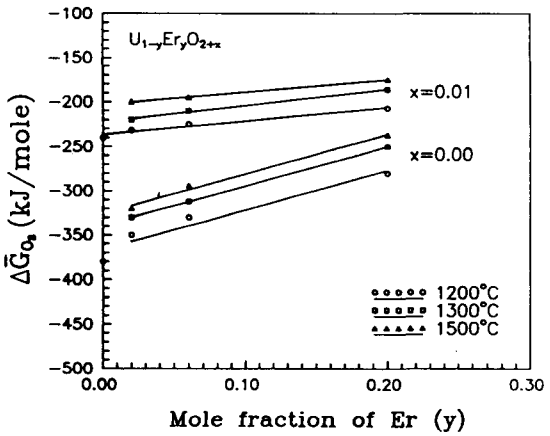

Fig. 6 Oxygen Potentials of $U_{1-y}Er_yO_{2+x}$ as a Function of Erbium Content.

The mean valence of uranium were calculated assuming the valences of erbium and oxygen in the specimen to be +3 and −2, respectively. The equilibrium among uranium ions and oxygen ions in UO_{2+x} and oxygen gas in the atmosphere is written as follows :

$$O^{2-} + 2U^{5+} = 2U^{4+} + {}^1/_2O_2(g). \qquad (3-5)$$

Application of the law of mass action to this equation yields

$$K = \frac{[U^{4+}]^2 p_{O_2}^{1/2}}{[U^{5+}]^2 [O^{2-}]}, \qquad (3-6)$$

where K is the equilibrium constant and square brackets is the concentration of each species per total cation site. When the composition of solid solution is taken as $U_{1-y}Er_yO_{2\pm x}$, the concentration of cation sites satisfies following equation

$$[U^{4+}] + [U^{5+}] = 1-y, \qquad (3-7)$$

and the electroneutrality condition requires

$$4[U^{4+}] + 5[U^{5+}] = V_U(1-y) \qquad (3-8)$$

and $$[O^{2-}] = 2+x = \frac{3}{2}y + \frac{1}{2}V_U(1-y) \qquad (3-9)$$

where V_U is the mean valence of the U ion. By substituting equations (3−7), (3−8) and (3−9) into (3−6),

$$\log p_{O_2} = 2\log K + 2\log[\frac{3}{2}y + \frac{1}{2}V_U(1-y)] + 4\log\frac{V_U-4}{5-V_U}. \qquad (3-10)$$

In the case of a combination of U^{4+} and U^{6+}, the corresponding equation is

$$\log p_{O_2} = 2\log K + 2\log[\frac{3}{2}y + \frac{1}{2}V_U(1-y)] + 2\log\frac{V_U-4}{6-V_U}. \qquad (3-11)$$

The variations of oxygen partial pressures with the mean uranium valence which is calculated by Eq. (3−9) at 1200, 1300 and 1500°C are shown in Fig. 7 for y=0.06 and in Fig. 8 for y=0.20, as a func-

tion of mean uranium valence. The change of p_{O_2} values with V_U has a similar trend with the case of $\Delta \overline{G}_{O_2}$ versus O/(U+Er) plots.

The p_{O_2} values calculated by Eq.(3−10) and Eq. (3−11) and the measured values as a function of V_U at 1200 and 1500°C are shown in Fig. 9 and Fig. 10, respectively. The measured values for pure UO_{2+x} are intermediate values between the U^{5+}/U^{4+} model and the U^{6+}/U^{4+} model as shown in Fig. 9. A complex model including the contribution of small amounts of U^{6+} in addition to U^{5+} is considered to meet with the best agreement in this case. In Fig. 10, the measured values for $U_{0.98}Er_{0.02}O_{2+x}$ at 1500°C are reasonably represented by the calculated curve from the U^{5+}/U^{4+} model.

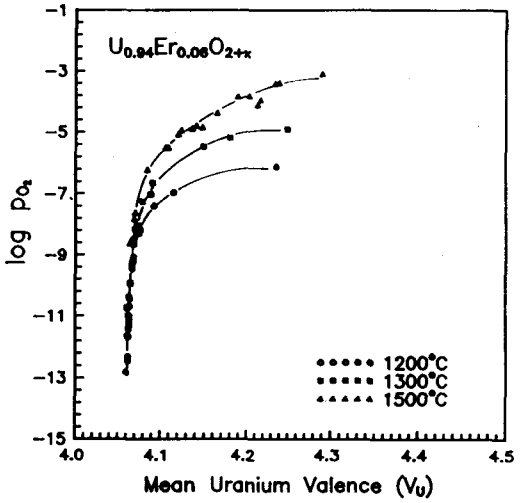

Fig. 7. Oxygen Partial Pressure versus Mean Uranium Valence for $U_{0.94}Er_{0.06}O_{2+x}$.

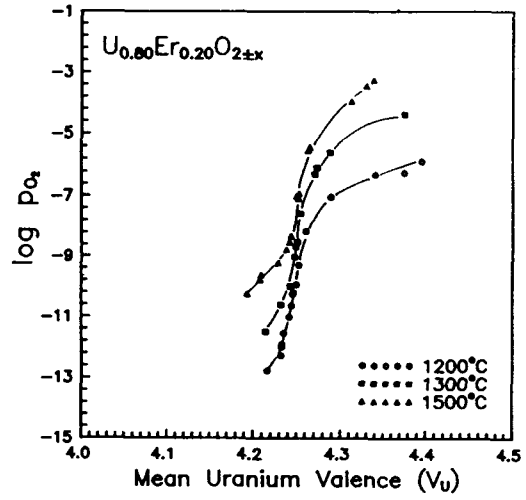

Fig. 8. Oxygen Partial Pressure versus Mean Uranium Valence for $U_{0.80}Er_{0.20}O_{2\pm x}$.

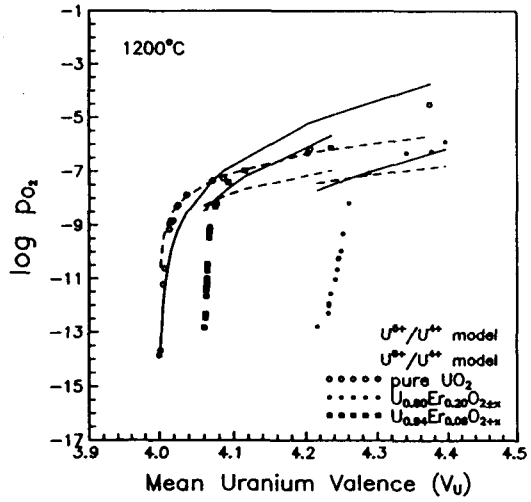

Fig. 9. Comparison of p_{O_2} between Measured Values and Calculated Values by Mean Uranium Valence Model for UO_{2+x} and $U_{0.80}Er_{0.20}O_{2\pm x}$ at 1200°C.

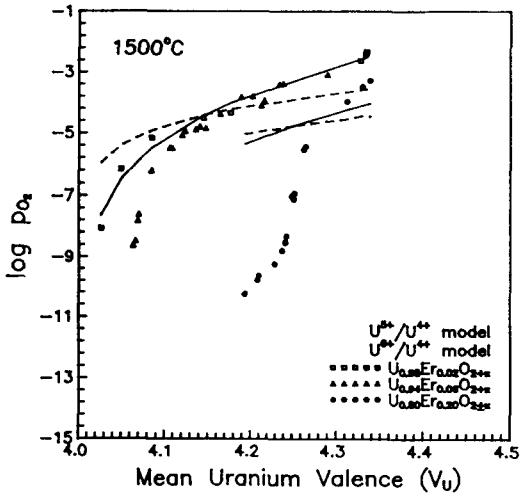

Fig. 10. Comparison of p_{O_2} between Measured Values and Calculated Values by Mean Uranium Valence Model for $U_{0.98}Er_{0.20}O_{2+x}$ and $U_{0.80}Er_{0.202\pm x}$ at 1500°C.

Yamashita and Fujino [27] have studied the phase behavior of $U_{1-y}Ca_yO_{2+x}$ solid solution, and observed two types of charge compensation ; in the range $0 \leq y \leq 0.1$, uranium valence remains unchanged but the O/(U+Ca) ratio linearly decreases with increasing y. In the range $0.2 \leq y \leq 0.33$, on the other hand, U^{4+} atoms in the solid solution are oxidized to the higher states. It means that the concentration of oxygen vacancy increases for $y \leq 0.1$, the concentration of positive polaron increases for higher dopant content in order to compensate the charge valence with increasing of y. However, introduction of trivalent ion necessitates some U ions having higher charges than U^{4+} as positive holes or additional negative charges from excess interstitial oxygens are compensated for by U ions only. The mean valence of uranium of +5 is a major factor which determines the single phase limit of the fcc solid solution [27]. Fig. 2 has shown that the lattice parameters of the solid solutions contract as the dopant content increases that means the mean uranium valence increases from +4 to higher value.

However, the measured values for $U_{0.94}Er_{0.06}O_{2\pm x}$ and $U_{0.80}Er_{0.20}O_{2\pm x}$ never approach to the calculated values based on both the U^{5+}/U^{4+} model and the U^{6+}/U^{4+} model, as shown in Fig. 9 and Fig. 10. It is considered, on the contrary on the results for $U_{1-y}Gd_yO_{2+x}$ [26], that the oxygen potentials for $U_{1-y}Er_yO_{2\pm x}$ solid solutions cannot be determined by the mean uranium valence alone. It means that the oxygen potentials cannot be interpreted by the mean uranium valence model if dopant content is increased. It is caused by that the interactions among defects may play an important role for defining the oxygen potentials in solid solutions.

4. Conclusions

The lattice parameter of the $U_{1-y}Er_yO_2$ solid solution decreases linearly with the increase of dopant content in the range of $y=0$ to $y=0.33$. The linear equation was expressed as $a(\text{Å}) = 5.4695 - 0.220y$, $(0 \leq y \leq 0.33)$. The experimental coefficient of $y = -0.220$ in $U_{1-y}Er_yO_2$ was an intermediate value between the calculated values -0.273 and -0.156 for the oxidation state of U^{5+} and U^{6+}, respectively.

$\Delta \overline{G}_{O_2}$ of $U_{1-y}Er_yO_{2\pm x}$ solid solutions increases as increasing y and/or equilibrium temperature at a given oxygen composition. The $\Delta \overline{G}_{O_2}$ has been found to undergo a abrupt increase in the range of -360 to -270 kJ/mole for $y=0.06$ and -320 to -220 kJ/mole for $y=0.20$, respectively in the temperature range of 1200~1500°C.

The oxygen potentials for UO_{2+x} can be expressed by the mean uranium valence model which includes the contribution of the U^{6+}/U^{4+} model in addition to the U^{5+}/U^{4+} model. Meanwhile, the oxygen potentials cannot be interpreted by the mean uranium model for $y \geq 0.06$ in $U_{1-y}Er_yO_{2\pm x}$.

References

1. L.V.C. Corsetti, S.C. Hatfield and A. Jonsson, International Topical Meeting on Fuel performance, Avignon-France, April 21−24, 1991
2. O.T.Sørensen, in Nonstoichiometric Oxides, eds. A.S. Nowick and G.G. Libowitz p50, Academic Press (1981)
3. C.R.A. Catlow, J. Nucl. Mater., 67, 236 (1977)
4. K. Park and D.R. Olander, High Temp. Science, 29, 203 (1990)
5. N.J. Dudney, R.L. Coble and H.L. Tuller, J. Am. Ceram. Soc., 64, 627 (1981)
6. T. Matsui and K. Naito, J. Nucl. Mater., 138, 19 (1986)
7. T.B. Lindemer and J. Brynestad, J. Am. Ceram. Soc., 69, 869 (1986)
8. T.L. Markin and E.C. Crouch, J. Inorg. Nucl. Chem., 32, 77 (1970)
9. T. Yamashita and T. Fujino, J. Nucl. Mater., 132, 192 (1985)
10. K. Une and M. Oguma, J. Nucl. Mater., 118, 189 (1983)
11. S. Fukushima, T. Ohmichi et al., J. Nucl. Mater.,

114, 312 (1983)
12. T. Fujino et al., J. Nucl. Mater., 174, 92 (1990)
13. T. B. Lindemer and A. L. Sutton, Jr., J. Am. Ceram. Soc., 71, 553 (1988)
14. K. Une and M. Oguma, J. Nucl. Mater., 115, 84 (1983)
15. K. Une and. M. Oguma, J. Nucl. Mater., 131, 88 (1985)
16. T. Matsui and K. Natio, J. Nucl. Mater., 132, 212 (1985)
17. T. B. Lindemer and T.M. Besmann J. Nucl. Mater., 130, 473 (1985)
18. R.E. Woodley, J. Nucl. Mater., 96, 5 (1981)
19. J. Edwards, R.N. Wood and G.R. Chilton, J. Nucl. Mater., 130, 505 (1985)
20. H.S. Kim, Y.K. Yoon and M.S. Yang, J. Nucl. Mater., 209, 286 (1994)
21. T. Ohmichi et al., J. Nucl. Mater., 102, 40 (1981)
22. R.J. Beals and J.H. Handwerk, J. Am. Ceram. Soc., 48, 271 (1965)
23. R.D. Shannon, Acta Cryst., A32, 751 (1976)
24. M. Sugisaki and T. Sueyoshi, J. Inorg. Nucl. Chem., 40, 1543 (1978)
25. J. Tateno, T. Fujino and H. Tagawa, J. Solid State Chem., 30, 265 (1979)
26. K. Une and M. Oguma, J. Nucl. Mater., 110, 215 (1982)
27. T. Yamashita and T. Fujino, J. Nucl. Mater., 136, 117 (1985)